Biochem J. Author manuscript; available in PMC 2008 September 01.

Published in final edited form as:
Biochem J. 2008 March 1; 410(2): 359–368. doi:10.1042/BJ20071138.

Peroxiredoxins play a major role in protecting *Trypanosoma cruzi* against macrophage- and endogenously-derived peroxynitrite

Lucía Piacenza[*], **Gonzalo Peluffo**[*], **María Noel Alvarez**[*], **John M. Kelly**[†], **Shane R. Wilkinson**[†], and **Rafael Radi**[*,1]

[*]Departamento de Bioquímica and Center for Free Radical and Biomedical Research, Facultad de Medicina, Universidad de la República, Montevideo, Uruguay

[†]Department of Infectious and Tropical Diseases, London School of Hygiene and Tropical Medicine, London, WC1E 7HT, U.K.

Abstract

There is increasing evidence that *Trypanosoma cruzi* antioxidant enzymes play a key immune evasion role by protecting the parasite against macrophage-derived reactive oxygen and nitrogen species. Using *T. cruzi* transformed to overexpress the peroxiredoxins TcCPX (*T. cruzi* cytosolic tryparedoxin peroxidase) and TcMPX (*T. cruzi* mitochondrial tryparedoxin peroxidase), we found that both cell lines readily detoxify cytotoxic and diffusible reactive oxygen and nitrogen species generated *in vitro* or released by activated macrophages. Parasites transformed to overexpress TcAPX (*T. cruzi* ascorbate-dependent haemoperoxidase) were also more resistant to H_2O_2 challenge, but unlike TcMPX and TcCPX overexpressing lines, the TcAPX overexpressing parasites were not resistant to peroxynitrite. Whereas isolated tryparedoxin peroxidases react rapidly ($k = 7.2 \times 10^5\ M^{-1} \cdot s^{-1}$) and reduce peroxynitrite to nitrite, our results demonstrate that both TcMPX and TcCPX peroxiredoxins also efficiently decompose exogenous- and endogenously-generated peroxynitrite in intact cells. The degree of protection provided by TcCPX against peroxynitrite challenge results in higher parasite proliferation rates, and is demonstrated by inhibition of intracellular redox-sensitive fluorescence probe oxidation, protein 3-nitrotyrosine and protein-DMPO (5,5-dimethylpyrroline-*N*-oxide) adduct formation. Additionally, peroxynitrite-mediated over-oxidation of the peroxidatic cysteine residue of peroxiredoxins was greatly decreased in TcCPX overexpressing cells. The protective effects generated by TcCPX and TcMPX after oxidant challenge were lost by mutation of the peroxidatic cysteine residue in both enzymes. We also observed that there is less peroxynitrite-dependent 3-nitrotyrosine formation in infective metacyclic trypomastigotes than in non-infective epimastigotes. Together with recent reports of up-regulation of antioxidant enzymes during metacyclogenesis, our results identify components of the antioxidant enzyme network of *T. cruzi* as virulence factors of emerging importance.

Keywords

cytosolic peroxiredoxin; macrophages; mitochondrial peroxiredoxin; peroxynitrite; *Trypanosoma cruzi*; virulence

[1] To whom correspondence should be addressed (email rradi@fmed.edu.uy)..

Europe PMC Funders Author Manuscripts

INTRODUCTION

Chagas disease affects 18-20 million people in Latin America and is caused by the kinetoplastida protozoan *Trypanosoma cruzi* [1]. This parasite undergoes extensive morphological and biochemical changes during its life cycle. Non-infective epimastigotes proliferate in the gut of the insect vector (triatomid hematophage arthropod), where they differentiate into metacyclic trypomastigotes, the infective form for the vertebrate host. Once in the dermal layers or conjunctival mucosa, the trypomastigotes invade host cells, mainly macrophages, where they transform into amastigotes, the infective replicative intracellular stage [2]. After several cycles of binary division, transformation to trypomastigotes and host-cell disruption occurs [3]. Subsequently, infective forms access the bloodstream and penetrate other nucleated cells such as myocardiocytes, smooth muscle cells and astrocytes [4].

To establish an infection, metacyclic trypomastigotes must invade macrophages and survive the highly oxidative conditions generated inside the phagosome. Several antioxidant enzymes, including a mitochondrial Fe-SOD (iron-containing superoxide dismutase), TcMPX (*T. cruzi* mitochondrial tryparedoxin peroxidase) and TcAPX (*T. cruzi* ascorbate-dependent haemoperoxidase), are upregulated during transformation of the insect-derived non-infective epimastigotes into the infective metacyclic trypomastigotes [5]. These biochemical changes may pre-adapt metacyclic forms with the capacity to detoxify reactive oxygen and nitrogen species generated by the macrophage during the *T. cruzi*-mammalian host-cell interactions [5].

Peroxide detoxification in trypanosomatids, including *T. cruzi*, relies on a sophisticated system of linked pathways in which the dithiol $T(SH)_2$ (trypanothione; N^1,N^8-bisglutathionylspermidine), the flavoenzyme TR (trypanothione reductase) and the thioredoxin homologue tryparedoxin play central roles as the major donors of reducing equivalents derived from NADPH [6,7]. Five distinct peroxidases have been identified in *T. cruzi* which differ in their subcellular location and substrate specificity. Two of these peroxidases, TcGPX [*T. cruzi* GPX (glutathione-dependent peroxidase)] I and TcGPXII, have sequence similarity with non-selenium GPXs. TcGPXI is localized to the cytosol and the glycosome, whereas TcGPXII is localized to the endoplasmic reticulum. Transformation-mediated overexpression of both enzymes confers resistance against exogenous hydroperoxides [8,9]. TcCPX (*T. cruzi* cytosolic tryparedoxin peroxidase) and TcMPX belong to the 2-cysteine peroxiredoxin family, which have the capacity to detoxify H_2O_2, peroxynitrite [10] and small-chain organic hydroperoxides [11]. In the corresponding transformed cell lines, overexpressed TcCPX is localized to the cytosol and TcMPX is localized exclusively to mitochondria. Total $T(SH)_2$-dependent peroxidase activity in these trypanosomes was 2.5- and 1.9-fold higher respectively than in wild-type parasites, with elevated levels of the peroxiredoxins conferring protection against exogenous peroxides (H_2O_2 and *t*-butyl-hydroperoxide), but no protective effects were found against the trypanocidal drugs nifurtimox and benznidazole, agents that are thought to undergo redox cycling within the cell [11]. A fifth peroxidase, TcAPX, is located in the endoplasmic reticulum. Overexpression of this enzyme resulted in a 5-fold increase in terms of activity and also conferred resistance against H_2O_2 challenge [12]. In addition, *T. cruzi* contains a repertoire of four Fe-SODs, which are located in different subcellular compartments, to detoxify $O_2^{\bullet -}$. Mitochondrial Fe-SOD overexpression interferes with the mitochondrial $O_2^{\bullet -}$-dependent signalling of *T. cruzi* programmed cell death induced by fresh human serum [13].

During phagocytosis of parasites, macrophage membrane-associated NADPH oxidase is activated, resulting in the generation of $O_2^{\bullet -}$. Inside the phagosome, this is converted into

H_2O_2, and through the action of transition metals, to $^{\bullet}OH$ [14]. $^{\bullet}NO$, produced by iNOS (inducible NO synthase), can diffuse and rapidly react with $O_2^{\bullet-}$ in a diffusion-controlled reaction to form peroxynitrite, a strong oxidizing and cytotoxic effector molecule against *T. cruzi* [15]. Peroxynitrite ($pK_a = 6.8$) is partially protonated at pH 7.4 to peroxynitrous acid, which, after homolysis, produces the one-electron oxidant $^{\bullet}OH$ and $^{\bullet}NO_2$. The major reactivity of peroxynitrite *in vivo* involves the oxidation of thiol groups [16]. Peroxynitrite also nitrates tyrosine residues in proteins by a two-step process, where the initial reaction is the oxidation of tyrosine (by one-electron oxidants) to form a tyrosyl radical which in turns adds $^{\bullet}NO_2$ to yield 3-nitrotyrosine. In this context, the effectiveness of the parasite oxidative defence system at the onset of macrophage invasion is critical for successful infection. The reactivity of TcCPX against peroxynitrite has been evaluated *in vitro*. The enzyme catalytically reduces peroxynitrite to nitrite through a fast-reacting thiol group located at the peroxidatic cysteine residue (Cys^{52} and Cys^{81} in TcCPX and TcMPX respectively), thus acting as tryparedoxin/peroxynitrite oxidoreductases [10]. Although the capability of these peroxiredoxins to detoxify peroxynitrite is well defined *in vitro*, there is less information available on the *in vivo* relevance of tryparedoxin-dependent detoxification of macrophage-derived oxidants and the effect on the outcome of cell invasion.

In this present paper, we describe the parasite response to peroxynitrite challenge using *T. cruzi* epimastigotes and metacyclic trypomastigotes transformed to overexpress TcMPX, TcCPX or TcAPX. The results clearly demonstrate that both TcCPX and TcMPX act *in vivo* as peroxynitrite oxidoreductases, conferring major protection against this oxidant.

EXPERIMENTAL

Parasites

T. cruzi epimastigotes (CL-Brener, wild-type) were cultured at 28°C in BHI (brain heart infusion) medium [17]. Parasites overexpressing TcCPX, TcMPX or TcAPX were obtained as described previously [11,12]. The complete gene sequences of the enzymes were cloned into the trypanosomal vector pTEX-9E10 (Invitrogen) and a ligation was performed to insert a c-Myc-derived epitope (9E10) in frame at the 3′ end of the genes to produce the construct pTEX-enzyme-9E10 [11]. Transformed TcCPX, TcMPX and TcAPX cells were cultured in BHI medium containing 250 $\mu g \cdot ml^{-1}$ of geneticin (Sigma).

Site-directed mutagenesis

Oligonucleotide-directed *in vitro* mutagenesis was performed using the Stratagene QuikChange® mutagenesis kit, following the manufacturer's instructions. Briefly, amplifications were performed in a final volume of 50 μl, with pTEX-TcMPX-9E10 or pTEX-TcCPX-9E10 [8] used as the template DNA. The PCR parameters were as follows: 1 cycle of 95°C for 30 s, followed by 95°C for 30 s, 55°C for 1 min and 68°C for 6 min for 16 cycles. DpnI (10 units, Invitrogen) was then added to digest parental double-stranded DNA. The DpnI-digested PCR product (1 μl) was used to transform *Escherichia coli* XL1-Blue supercompetent cells. The primers used to generate each of the desired mutations were produced by MWG Biotech AG (Ebersberg, Germany) and are as follows: TcCPX C52A(F), 5′-GACTTCACCTTCGTCGCCCCCACAGAGATCTGC-3′; TcCPX C52A(R), 5′-GCAGATCTCTGTGGGGGCGACGAAGGTGAAGTC-3′; TcMPX C81A(F), 5′-GATTTTACCTTTGTGGCCCCCACAGAAATCACA-3′ and TcMPX C81A(R), 5′-TGTGATTTCTGTGGGGGCCAGAAAGGTAAAATC-3′. The relevant substitution sites, incorporating the required base changes, are underlined. Successful mutagenesis was confirmed by sequencing using a BigDye® terminator cycle sequencing kit (Applied Biosystems) and an ABI PRISM® 3730 automated sequencer (Applied Biosystems).

In vitro metacyclogenesis of *T. cruzi* CL-Brener and transformed cells

Epimastigotes were collected by centrifugation at 800 ***g*** for 10 min at 25°C and washed three times in 10 ml TAU (triatomine artificial urine) [190 mM NaCl, 17 mM KCl, 2 mM $MgCl_2$, 2 mM $CaCl_2$, 8 mM sodium phosphate buffer (pH 6.0) and 0.035 % sodium bicarbonate] and resuspended at (3-5) × 10^8 cells · ml^{-1}. After incubation at 28°C for 2 h, the parasites were transferred and diluted in TAU3AAG (TAU three amino acids plus glucose) medium [TAU (pH 6.0) supplemented with 10 mM L-proline, 50 mM sodium L-glutamate, 2 mM sodium L-aspartate and 10 mM glucose to (3-5) × 10^6 cells · ml^{-1}, following incubation for 96 h at 28°C as described previously [18].

Oxidant-sensitivity experiments

Epimastigotes (3 × 10^8 cells · ml^{-1}) were incubated for 1 h at 28°C in DPBS (Dulbecco's PBS, pH 7.3; Sigma), and 0-800 μM H_2O_2 and peroxynitrite (synthesized from sodium nitrite and H_2O_2 in acidic medium using a quenched flow reactor as described previously [19]). Peroxynitrite (0-1000 μM) was added with vigorous vortex-mixing to parasite suspensions as a single or multiple doses of 100 μM, reaching the different final concentrations as indicated. $O_2^{\bullet-}$ was generated using the redox-cycling compound 50 μM DMNQ (2,3-dimethoxy-1-naphthoquinone; Sigma) (5 nM $O_2^{\bullet-}$/1 × 10^8 cells per min), estimated from H_2O_2 formation by the *p*-hydroxyphenyl acetic acid/horseradish peroxidase assay [13,20]. AA (antimycin A) (5 μM; Sigma)-treated epimastigotes were used to elicit mitochondrial-derived $O_2^{\bullet-}$ generation [21,22]. $^{\bullet}$NO fluxes were generated by NO donors, 0-1 mM spermine NONOate (diazeniumdiolate, $t_{1/2}$ ~45 min; Alexis) and 0-2 mM NOC-18 ($t_{1/2}$ ~1080 min, Alexis), and quantified following the oxidation of oxyhaemoglobin to methaemoglobin at 577 nm (ε_{577} = 11 mM^{-1} · cm^{-1}) [23]. Parasites were incubated in the presence of the different oxidant-generating systems for 1 h at 28°C in DPBS (pH 7.3).

Macrophage-derived oxidants

The murine macrophage cell line J774A.1 was cultured in DMEM (Dulbecco's modified Eagle's medium; Sigma) at 37°C in a 5 % CO_2 atmosphere. Production of $^{\bullet}$NO by iNOS was triggered by pre-incubating macrophages with 300-500 units · ml^{-1} IFNγ (interferon γ; Calbiochem) and 3 μg · ml^{-1} lipopolysaccharide (Sigma) for 5 h at 37°C for maximal $^{\bullet}$NO production [15]. $O_2^{\bullet-}$ production by NADPH oxidase in macrophages was triggered by the addition of 2 μg · ml^{-1} PMA (Sigma) as described previously [15]. Macrophage/*T. cruzi* co-culture experiments were performed at 37°C by direct contact of parasites with the macrophage monolayer, allowing cell-to-cell interactions. Cells were then harvested and assayed for [^{3}H]thymidine (American Radiolabeled Chemicals, St Louis, MO, U.S.A.) incorporation [17] and RH (rhodamine) 123 fluorescence [15]. After iNOS induction, 2 μg · ml^{-1} PMA was added to macrophages 5 min before parasite addition, and co-culture experiments were performed for 90 min at 37°C.

Assessment of parasite viability

After treatment, parasite viability was evaluated using the [^{3}H]thymidine incorporation assay as described previously [17]. Briefly, following parasite exposure to the different oxidative systems, an aliquot containing 5 × 10^6 cells was incubated overnight at 28°C in BHI medium containing 1 μCi [^{3}H]thymidine. When transformed parasites were used, BHI medium was supplemented with 250 μg · ml^{-1} of geneticin. Results are the percentage of [^{3}H]thymidine incorporation compared with the control (no oxidant addition) sample for each cell line (wild-type and TcAPX, TcCPX or TcMPX overexpressing cells). The IC_{50} values for H_2O_2 and peroxynitrite were calculated to be the oxidant concentration that produced a 50 % inhibition in the [^{3}H]thymidine incorporation assay compared with the control sample.

DHR (dihydrorhodamine) oxidation

Parasites (1×10^9 cells $\cdot$ ml^{-1}) were incubated for 30 min at 28°C in DPBS containing 50 μM DHR (Molecular Probes). After incubation, cells were centrifuged at 800 ***g*** for 10 min at 25°C and washed twice in DPBS in order to eliminate non-incorporated DHR. Detection of intracellular RH 123, the oxidation product of DHR, was performed after exposure to the different experimental conditions (oxidant and macrophage-derived oxidant treatment) using black 96-well plates and a fluorescence plate reader at 28°C (Fluostar; BMG Labtech, Offenburg, Germany), with filters set at λ_{ex} = 485 nm and λ_{em} = 520 nm. In order to evaluate membrane integrity and parasite morphology after peroxynitrite addition, cells were pre-loaded for 30 min with 10 μM 6-CFDA (6-carboxyfluorescein diacetate; Molecular Probes) and washed three times in DPBS. After exposure to 250 μM peroxynitrite, parasites were examined by fluorescence microscopy (Nikon Eclipse TE-200 inverted microscope) and digital images of treated parasites were recorded.

Peroxynitrite-mediated oxidative modifications to proteins

Parasites were exposed to 0-1 mM peroxynitrite as described above. After treatment, cells were centrifuged at 800 ***g*** for 10 min at 25°C, resuspended in 250 μl lysis buffer [10 mM Tris/HCl (pH 8.0), 1 mM EDTA and 0.5 % Triton X-100] and incubated on ice for 15 min. Cell extracts were centrifuged at 13 000 ***g*** for 30 min at 4°C, and loading buffer [30 mM Tris/HCl (pH 6.6), 1 % SDS and 5 % (v/v) glycerol] was added to the supernatants. Proteins (50 μg) were resolved by SDS/PAGE (13 % gels), followed by Western blotting on to nitrocellulose membranes. After protein transfer, membranes were stained with Ponceau-S solution (Applichem, Darmstadt, Germany) to confirm equal protein loading. The membranes were blocked using 5 % (w/v) BSA and 0.1 % Tween 20 (Sigma) in TBS (Tris-buffered saline) [25 mM Tris/HCl (pH 7.4), 140 mM NaCl and 3 mM KCl] for 1 h at 25°C. The membranes were then probed with rabbit anti-(nitrotyrosine) serum (1:2000 dilution) [24], rabbit anti-(sulfonic peroxiredoxin) antibody (1:2000 dilution; Lab Frontier, Seoul, Korea) that recognizes cysteine sulfinic acid (Cys-SO_2H) and sulfonic acid (Cys-SO_3H) from human peroxiredoxin I to IV [25] and monoclonal mouse anti-c-Myc antibody (9E10, 1:300 dilution; Santa Cruz Biotechnology) for 1 h at 25°C. Immunoreactive proteins were detected using the Immun-Star™ chemiluminescence kit (Bio-Rad). Immunodetection of DMPO (5,5-dimethylpyrroline-*N*-oxide)-nitrone protein adducts on parasite samples was performed using a rabbit anti-(DMPO-nitrone) serum which binds to the one-electron oxidation product of the initial DMPO-nitroxyl protein spin adduct [26]. Parasites (1×10^9 cells $\cdot$ ml^{-1}) were pre-incubated with DMPO (100 mM) in DPBS for 30 min at 28°C. After incubation, parasites were collected by centrifugation at 800 ***g*** for 10 min at 25°C and resuspended at a concentration of 3×10^8 cells $\cdot$ ml^{-1} in DPBS. After peroxynitrite treatment, parasite extracts were prepared as above and protein extracts (50 μg) were resolved by SDS/PAGE (12 % gels), blotted on to nitrocellulose and probed with anti-(DMPO-nitrone) serum (1:2000 dilution) as described previously [26]. Immunoreactive proteins were detected using the Immun-Star™ chemiluminescence kit (Bio-Rad).

Data analysis

All results are means ± S.D. unless otherwise stated. For comparison between two groups, the Student's *t* test was performed. ANOVA was performed for comparison of more than two groups. Post-hoc analysis was performed using a LSD (least significant difference) test. $P < 0.05$ was considered significant. All experiments were typically repeated on separate days ($n \geq 3$).

RESULTS

Transformed *T. cruzi* overexpressing TcAPX, TcMPX or TcCPX show differential susceptibility to hydrogen peroxide and peroxynitrite

In order to evaluate the susceptibility of the genetically transformed *T. cruzi* parasite lines to H_2O_2, cells were exposed to different concentrations of oxidant for 1 h and parasite viability was assayed. *T. cruzi* epimastigotes overexpressing TcAPX showed a 2-fold increase in their IC_{50} value compared with wild-type cells, whereas cells with elevated levels of TcMPX and TcCPX were 50 % more resistant to oxidant exposure (Table 1). Expression of the appropriate peroxidase in each transformed cell line was confirmed by the detection of the c-Myc tag epitope in parasite extracts (Figure 1).

Unlike with H_2O_2, TcAPX overexpression did not confer protection against peroxynitrite (Figure 2A), with an IC_{50} value comparable with wild-type cells (250 ± 25 and 280 ± 12 μM respectively; Table 1). In contrast, overexpression of TcMPX or TcCPX conferred resistance against peroxynitrite when added exogenously as a single dose (Table 1). The dose-response curve showed a biphasic profile for both cell lines overexpressing the peroxiredoxins (Figures 2B and 2C), suggesting there is a marked resistance at the lower concentration range tested, particularly for cells with elevated levels of TcCPX (Figure 2C). The major difference between wild-type and *T. cruzi* overexpressing TcCPX was observed at 400 μM peroxynitrite (90 % compared with 20 % inhibition of [^{3}H]thymidine incorporation respectively). At higher peroxynitrite doses (≥500 μM), proliferation was inhibited in all cell lines. When these experiments were extended to investigate cellular responses to the consecutive addition of sub-lethal levels of peroxynitrite (100 μM) at 1 min intervals, parasites overexpressing TcCPX or TcMPX displayed remarkable resistance, greater than the resistance observed during the addition of a single dose (Figure 2D). Peroxiredoxins depend on a trypanothione redox cascade and, ultimately, on NADPH arising from the pentose phosphate pathway, which is stimulated after oxidant addition [13] in order to regenerate the active enzyme form. Therefore the time between each challenge allows TcCPX and TcMPX to be in the reduced-active state prior to the next oxidant assault.

Examination of cell morphology after peroxynitrite challenge (250 μM) revealed that wild-type cells lost their cellular structure, whereas parasites overexpressing TcCPX appeared to be unaffected (Figure 2E). The activity of both trypanosomal peroxiredoxins is dependent on a conserved peroxidatic cysteine residue at positions 52 and 81 in TcCPX and TcMPX respectively [10]. To investigate whether these residues play a key role in the metabolism of peroxynitrite, they were mutated to alanine residues, in order to yield inactive enzymes. The mutated enzymes were expressed at similar levels to that shown in Figure 1 for the wild-type form (results not shown). Parasites expressing TcCPX C52A and TcMPX C81A failed to confer peroxynitrite resistance, demonstrating the catalytic nature of the protection afforded by elevated levels of wild-type peroxiredoxins (inset, Figure 2C).

Overexpression of *T. cruzi* peroxiredoxins inhibits peroxynitrite-induced oxidative modifications

By metabolising peroxynitrite, peroxiredoxins play a key role in minimising the formation of peroxynitrite-derived radicals such as $^{\bullet}OH$, $^{\bullet}NO_2$ and $CO_3^{\bullet-}$ [10]. To determine whether parasites overexpressing TcCPX or TcMPX have decreased levels of peroxynitrite-derived radicals, cells were pre-loaded with the redox sensitive agent DHR (which is oxidized to RH 123, a fluorescent product) and then challenged with the oxidant [15]. Overexpression of either TcMPX or TcCPX resulted in partial inhibition (~50 %) of intracellular DHR oxidation in a dose-dependent manner compared with wild-type cells (Figure 3A). In

contrast, *T. cruzi* overexpressing TcAPX displayed a fluorescence pattern similar to controls (results not shown).

Peroxynitrite-dependent oxidative modification of proteins was analysed by immunospin-trapping using an anti-(DMPO-nitrone) serum [27]. Intense immunostaining was observed in CL-Brener epimastigotes after peroxynitrite treatment, whereas only minimal staining was observed in TcCPX or TcMPX overexpressing cells (Figure 3B). Moreover, basal levels of modified proteins were higher in the control than in the overexpressing cells, suggesting that there are lower steady-state levels of endogenous oxidants in the overexpressing cells. The inhibition of peroxynitrite-dependent protein modifications in cells with elevated TcCPX was further confirmed by blotting for tyrosine nitration (Figure 3C).

Finally, peroxynitrite-mediated two-electron thiol oxidation processes lead to the formation of sulfenic acid, which forms an intersubunit disulfide bond at the expense of the resolving cysteine residue of the enzyme, which can then be reduced at the expense of tryparedoxin. Under conditions of excess oxidant, the peroxiredoxin catalytic thiol present in the sulfenic state can be over-oxidized to sulfinic and sulfonic acid derivatives, before reacting with the resolving cysteine residue [28,29]. Detection of sulfinic and/or sulfonic acid at the active site of TcCPX was performed immunochemically after exposure to different peroxynitrite doses [25]. In wild-type parasites exposed to peroxynitrite, over-oxidized peroxiredoxins were detected, including some staining under basal conditions. Importantly, we could not detect over-oxidation of peroxiredoxins in cells overexpressing TcCPX incubated with up to 1 mM peroxynitrite, with only minor staining at higher concentrations (2 mM) (Figure 3D).

Enhanced resistance of TcMPX or TcCPX overexpressing cells against mitochondrial and cytosolic generation of peroxynitrite

To evaluate the protection conferred by TcMPX or TcCPX overexpression against intracellularly-formed peroxynitrite, the viability of parasites treated with compounds known to stimulate cytosolic (DMNQ) or mitochondrial (AA) $O_2^{\bullet -}$ formation in the presence of different $^{\bullet}NO$ fluxes (in order to have defined ratios of both oxidants) was examined as described in the Experimental section [13,21]. For the mitochondrial $O_2^{\bullet -}$ generating system, AA alone was toxic to wild-type cells, as a result of intramitochondrial $O_2^{\bullet -}$ and/or subsequent intracellular H_2O_2 formation [30,31], a feature that was decreased in both TcCPX and TcMPX overexpressing trypanosomes. When AA-treated cells were also exposed to $^{\bullet}NO$ fluxes (NOC-18, 0-0.25 μM $^{\bullet}NO \cdot min^{-1}$), overexpression of TcMPX was found to have significantly improved [^{3}H]thymidine incorporation with respect to TcCPX and wild-type cells, indicating that TcMPX minimizes the toxic growth effects of mitochondrially-generated peroxynitrite (Figures 4A and 4B). We then assayed for the production of peroxynitrite-derived radicals in intact cells loaded with DHR. In parasites overexpressing TcMPX, and to a minor extent TcCPX (results not shown), RH 123 formation was partially inhibited, giving further support to the idea that TcMPX plays an important role in detoxifying peroxynitrite generated within mitochondria (Figure 4C). When reciprocal experiments were performed using physiologically relevant cytosolic $O_2^{\bullet -}$ fluxes (5 nM $O_2^{\bullet -}/10^8$ cells $\cdot$ min^{-1}), a similar resistance was observed using trypanosomes expressing elevated levels of TcCPX (see Supplementary Figure 1 at http://www.BiochemJ.org/bj/410/bj4100359add.htm).

Finally, and of most relevance, epimastigotes were exposed to activated macrophages that produced $O_2^{\bullet -}$, $^{\bullet}NO$ or both, in a cell-to-cell contact model as described previously [15]. Simultaneous macrophage generation of $O_2^{\bullet -}$ and $^{\bullet}NO$ inhibited growth of wild-type and TcAPX overexpressing parasites by equivalent levels (Table 2) [15]. However, overexpression of TcMPX conferred partial protection against growth inhibition, and TcCPX overexpression completely protected cells against macrophage-derived peroxynitrite

(Table 2). Consistent with these results, intracellular oxidation of DHR in TcCPX or TcMPX overexpressing cells exposed to macrophage-derived $O_2^{\bullet -}$ and $^{\bullet}NO$ was greatly decreased compared with wild-type (results not shown).

Increased resistance of the infective metacyclic stage of *T. cruzi* against peroxynitrite

A recent proteomic study reported that components of the oxidative defence system appeared to be up-regulated during metacyclogenesis [5]. Using wild-type epimastigotes and chemically-differentiated wild-type metacyclic trypomastigotes, we evaluated protein 3-nitrotyrosine formation after peroxynitrite challenge. As shown in Figure 5(A), protein nitrotyrosine in wild-type metacyclic trypomastigotes was detected at a significantly decreased level than that observed in the epimastigote stage when treated with equal amounts of peroxynitrite. These results support, from a biochemical standpoint, the previously observed increase in the levels of antioxidant enzymes during the infective stage [5]. Parasites transformed to express elevated levels of TcCPX and TcMPX were also subjected to chemical differentiation to the infective metacyclic stage. The preservation of enzyme expression was corroborated by detection of the c-Myc-tagged enzyme by Western blot analysis (Figure 5B). Peroxynitrite treatment of the metacyclic parasites overexpressing TcCPX showed inhibition of protein 3-nitrotyrosine formation (Figure 5C), and the redox-active cysteine in the peroxiredoxin displayed a decreased level of oxidation to cysteine sulfinic and/or sulfonic acid (Figure 5D), supporting the key role of this enzyme in protection against peroxynitrite.

DISCUSSION

Macrophages are among the first cells to be invaded by *T. cruzi* and, as a consequence, parasites need to cope with macrophage-derived oxidants. Since the discovery of peroxiredoxins in trypanosomatids, H_2O_2 and small-chain organic hydroperoxides have been assigned as the preferential biological substrates for these enzymes [11,32-34]. A fast reaction constant of TcCPX with peroxynitrite has been reported previously, with a value of $7.2 \times 10^5\ M^{-1} \cdot s^{-1}$ at pH 7.4. Furthermore, in the presence of tryparedoxin, TcCPX was shown to catalytically decompose peroxynitrite [10]. Given the relevance of peroxynitrite production as an effector cytotoxic molecule against *T. cruzi* [15,19,35] and the *in vitro* kinetic considerations, we decided to evaluate the importance of TcCPX and TcMPX against peroxynitrite challenge in the intact cell.

To evaluate the protective effects of these enzymes against biologically-relevant oxidants, we conducted experiments using epimastigotes that overexpress TcCPX, TcMPX or TcAPX. Using an acute challenge of H_2O_2 (1 h incubation), we showed that TcAPX confers higher protection than TcCPX and TcMPX, as was demonstrated previously [11,12]. IC_{50} values for wild-type parasites and TcAPX overexpressing cells against peroxynitrite were not different (Table 1), suggesting that TcAPX does not play a significant role in the detoxification of exogenously-added peroxynitrite. Notably, overexpression of TcCPX or TcMPX conferred a high level of protection on epimastigotes against a broad range of peroxynitrite concentrations (0-200 μM and 0-400 μM for TcMPX and TcCPX overexpressing cells respectively) (Figures 2B and 2C). The observed protection was lost when the peroxidatic cysteine mutants of TcCPX and TcMPX were used (inset, Figure 2C). Together, our results demonstrate that peroxiredoxins efficiently detoxify peroxynitrite in cells and protect the parasites from the deleterious actions of this oxidant [36]. At higher peroxynitrite concentrations, the effect was less pronounced. This suggests that either direct inactivation of TcMPX and TcCPX by peroxynitrite occurs, owing to over-oxidation of the enzyme thiol group, or acute depletion of reducing equivalents (NADPH) occurs, ultimately derived from the pentose phosphate pathway, which would jeopardize the catalytic efficiency of the antioxidant system. Further experiments, involving the sequential addition

of low concentrations of peroxynitrite, showed an increase in the total peroxynitrite concentration that the enzymes have the capacity to overcome (0-1 mM for TcMPX or TcCPX overexpressing cells; Figure 2D). This strongly suggests that TcCPX and TcMPX catalytically decompose peroxynitrite in our *in vivo* system. Also, these results eliminate the suggestion of inactivation of the enzymes at peroxynitrite concentrations less than 1 mM (see below).

The cytotoxic effects of peroxynitrite against *T. cruzi* result from direct reactions with critical parasite targets, such as essential enzymatic thiol residues, and from the actions of the induced radicals $^{\bullet}OH$, $CO_3^{\bullet-}$ and $^{\bullet}NO_2$ [15,19,35]. We therefore explored radical-mediated damage by using probes and evaluating modifications of endogenous constituents known to react with these radicals. TcCPX or TcMPX overexpressing cells effectively decreased peroxynitrite-dependent intracellular DHR oxidation, protein radical formation (as evaluated by DMPO immuno-spin trapping) and protein 3-nitrotyrosine formation (Figures 3A-3C). The relatively decreased protection afforded by peroxiredoxin overexpression on DHR oxidation compared with the oxidation/nitration of the other tested molecular targets, as well as in cell viability, is explained by the fact that DHR readily diffuses out of the cell, and therefore some of the peroxynitrite-dependent redox chemistry on DHR occurs extracellularly. Additionally, dose-dependent over-oxidation of peroxiredoxin(s) to sulfinic and/or sulfonic acid was evident after peroxynitrite treatment of wild-type cells, indicating that basal levels of TcCPX in the epimastigote stage are not sufficient to detoxify peroxynitrite at the concentrations tested (Figure 3D). In cells with elevated TcCPX, over-oxidation of the enzyme was not detected at concentrations below 2 mM peroxynitrite, an observation which supports our suggestion that, in overexpressing cells, the effect of peroxynitrite does not result from enzyme inactivation at these concentrations.

In living systems, peroxynitrite arises from physiologically-generated $^{\bullet}NO$ and $O_2^{\bullet-}$ fluxes at different ratios, and oxidation/nitration yields are responsive to peroxynitrite formation rates in spite of the flux ratio [37]. *T. cruzi* can be challenged by high levels of mammalian cell-derived $^{\bullet}NO$ and of $O_2^{\bullet-}$ which can be formed either by activation of macrophage NADPH oxidase or by the $^{\bullet}NO$-dependent inhibition of the mitochondrial respiratory chain in the target cell [30,38]. Therefore peroxynitrite can also be formed in different cellular compartments (such as cytosol and mitochondria). In order to assess the antioxidant capabilities of TcCPX and TcMPX in their subcellular locations, we used a system which allowed site-directed generation of $O_2^{\bullet-}$ radicals in the presence of $^{\bullet}NO$ fluxes. The inhibition in proliferation of TcCPX overexpressing and wild-type cells exposed to $^{\bullet}NO$ fluxes alone were similar, while TcMPX overexpressing cells exhibited a greater level of proliferation (≃50 % compared with 20 % inhibition respectively) (Figure 4A). $^{\bullet}NO$ is a known inhibitor of mitochondrial cytochrome *c* oxidase. This leads to an increase in mitochondrial $O_2^{\bullet-}$ production and consequently to peroxynitrite formation in the vicinity of mitochondria, which could explain the effect of TcMPX overexpression on parasite proliferation. When $O_2^{\bullet-}$ is generated in the cytosol by the redox cycling agent DMNQ, overexpression of TcCPX affords maximal protection, whereas TcMPX overexpressing cells behaved similarly to wild-type cells (results not shown). The presence of the complex III respiratory chain inhibitor AA has profound effects on parasite proliferation, with 80 % and 40 % inhibition of thymidine incorporation in wild-type and overexpressing cells respectively (Figure 4B). In the presence of $^{\bullet}NO$ fluxes, enhanced levels of TcMPX sustained proliferation capabilities and inhibited peroxynitrite-dependent DHR oxidation, whereas TcCPX overexpressing cells displayed a progressive decrease in proliferation (Figures 4B and 4C). Together, these results identify the importance of the compartmentalized antioxidant defences in the parasite against localized oxidant formation.

In *Leishmania chagasi*, overexpression of cytosolic peroxiredoxin 1 partially improved parasite survival within naive macrophages [33]. Maximal peroxynitrite-dependent trypanocidal activity of macrophages, including human macrophages [39], is observed under iNOS induction and $O_2^{\bullet -}$ generation by NADPH oxidase after parasite engulfment [15]. We therefore tested the hypothesis that overexpression of TcCPX would render the parasites resistant to macrophage-derived peroxynitrite in co-culture experiments, as evaluated by proliferation and intra-parasite DHR oxidation assays. Under maximal macrophage stimulation conditions (production of both $^{\bullet}NO$ and $O_2^{\bullet -}$), a 50 % inhibition in parasite proliferation was found in the wild-type and TcAPX overexpressing cells, and 30 % in cells with elevated TcMPX levels. No cytotoxic effects were observed in cells overexpressing TcCPX, with the proliferation rates being the same as the untreated controls (Table 2). These results correlate well with the DHR oxidation assays, where maximal protection was observed in the TcCPX overexpressing cells (results not shown). Although levels of $^{\bullet}NO$ achieved by activated human macrophages are smaller than those observed with murine macrophages, several reports have indicated that the trypanocidal activity depends on $^{\bullet}NO$ production [39,40]. Finally, in order to validate our findings in the infective metacyclic stage of the parasite, we chemically transformed epimastigotes (wild-type, TcCPX or TcMPX overexpressing cells) and evaluated peroxynitrite-dependent protein oxidative modifications. In wild-type parasites, metacyclic trypomastigotes contained less protein 3-nitrotyrosine than epimastigotes, in agreement with the expected up-regulation of antioxidant defences in the infective stage (Figure 5A) [5]. We successfully differentiated parasites overexpressing TcMPX or TcCPX to the infective stage, while retaining the overexpression phenotype (Figure 5B). Overexpression of TcCPX in the infective metacyclic stage prevented peroxynitrite-dependent protein nitrotyrosine formation and over oxidation of peroxiredoxins (Figures 5C and 5D).

Peroxynitrite production inside the macrophage phagosome have been estimated to be sufficient to kill internalized trypanosomes [15,41]. In line with this, we anticipate that overexpression of TcCPX will render *T. cruzi* resistant to macrophage killing and therefore increase its virulence. In this present paper, we have extensively analysed the role of tryparedoxin peroxidases in *T. cruzi* epimastigotes and at the metacyclic stage by exposure to diverse peroxynitrite-generating systems. We provide evidence that supports the key role of parasite tryparedoxin peroxidases in defence against macrophage-derived and even endogenously produced peroxynitrite. The results we present, together with enhanced antioxidant defence observed in the infective metacyclic stage of the parasite, place the antioxidant network of *T. cruzi* as an emerging virulence factor.

Supplementary Material

Refer to Web version on PubMed Central for supplementary material.

Acknowledgments

We thank Dr Ronald Mason (National Institutes of Environmental Health Science, 111 T.W. Alexander Drive, Research Triangle Park, NC, U.S.A.) for DMPO and the anti-DMPO serum. This work was supported by a grant from the Howard Hughes Medical Institute (H.H.M.I.) and the International Centre of Genetic Engineering and Biotechnology (I.C.G.E.B.) to R.R. L.P. and M.N.A. were partially supported by a grant from the Fondo Clemente Estable and fellowships from the Programa de Desarrollo de las Ciencias Basicas (PEDECIBA), Uruguay. S.R.W. and J.M.K. were funded by The Wellcome Trust. R. R. is an International Research Scholar of the H.H.M.I.

Abbreviations used

AA antimycin A

BHI	brain heart infusion
6-CFDA	6-carboxyfluorescein diacetate
DHR	dihydrorhodamine
DMNQ	2,3-dimethoxy-1-naphthoquinone
DMPO	5,5-dimethylpyrroline-*N*-oxide
DPBS	Dulbecco's PBS
Fe-SOD	iron-containing superoxide dismutase
GPX	glutathione-dependent peroxidase
iNOS	inducible NO synthase
RH	rhodamine
TAU	triatomine artificial urine
TcAPX	*Trypanosoma cruzi* ascorbate-dependent haemoperoxidase
TcCPX	*T. cruzi* cytosolic tryparedoxin peroxidase
TcGPX	*T. cruzi* GPX
TcMPX	*T. cruzi* mitochondrial tryparedoxin peroxidase
$T(SH)_2$	trypanothione

REFERENCES

1. Barrett MP, Burchmore RJ, Stich A, Lazzari JO, Frasch AC, Cazzulo JJ, Krishna S. The trypanosomiases. Lancet. 2003; 362:1469–1480. [PubMed: 14602444]
2. Burleigh BA, Woolsey AM. Cell signalling and *Trypanosoma cruzi* invasion. Cell Microbiol. 2002; 4:701–711. [PubMed: 12427093]
3. Tan H, Andrews NW. Don't bother to knock-the cell invasion strategy of *Trypanosoma cruzi*. Trends Parasitol. 2002; 18:427–428. [PubMed: 12377585]
4. Da Mata JR, Camargos MR, Chiari E, Machado CR. *Trypanosoma cruzi* infection and the rat central nervous system: proliferation of parasites in astrocytes and the brain reaction to parasitism. Brain Res. Bull. 2000; 53:153–162. [PubMed: 11044591]
5. Atwood JA III, Weatherly DB, Minning TA, Bundy B, Cavola C, Opperdoes FR, Orlando R, Tarleton RL. The *Trypanosoma cruzi* proteome. Science. 2005; 309:473–476. [PubMed: 16020736]
6. Shames SL, Fairlamb AH, Cerami A, Walsh CT. Purification and characterization of trypanothione reductase from *Crithidia fasciculata*, a newly discovered member of the family of disulfide-containing flavoprotein reductases. Biochemistry. 1986; 25:3519–3526. [PubMed: 3718941]
7. Carnieri EG, Moreno SN, Docampo R. Trypanothione-dependent peroxide metabolism in *Trypanosoma cruzi* different stages. Mol. Biochem. Parasitol. 1993; 61:79–86. [PubMed: 8259135]
8. Wilkinson SR, Meyer DJ, Taylor MC, Bromley EV, Miles MA, Kelly JM. The *Trypanosoma cruzi* enzyme TcGPXI is a glycosomal peroxidase and can be linked to trypanothione reduction by glutathione or tryparedoxin. J. Biol. Chem. 2002; 277:17062–17071. [PubMed: 11842085]
9. Wilkinson SR, Taylor MC, Touitha S, Mauricio IL, Meyer DJ, Kelly JM. TcGPXII, a glutathione-dependent *Trypanosoma cruzi* peroxidase with substrate specificity restricted to fatty acid and phospholipid hydroperoxides, is localized to the endoplasmic reticulum. Biochem. J. 2002; 364:787–794. [PubMed: 12049643]
10. Trujillo M, Budde H, Pineyro MD, Stehr M, Robello C, Flohe L, Radi R. *Trypanosoma brucei* and *Trypanosoma cruzi* tryparedoxin peroxidases catalytically detoxify peroxynitrite via oxidation of fast reacting thiols. J. Biol. Chem. 2004; 279:34175–34182. [PubMed: 15155760]

11. Wilkinson SR, Temperton NJ, Mondragon A, Kelly JM. Distinct mitochondrial and cytosolic enzymes mediate trypanothione-dependent peroxide metabolism in *Trypanosoma cruzi*. J. Biol. Chem. 2000; 275:8220–8225. [PubMed: 10713147]
12. Wilkinson SR, Obado SO, Mauricio IL, Kelly JM. *Trypanosoma cruzi* expresses a plant-like ascorbate-dependent hemoperoxidase localized to the endoplasmic reticulum. Proc. Natl. Acad. Sci. U.S.A. 2002; 99:13453–13458. [PubMed: 12351682]
13. Piacenza L, Irigoin F, Alvarez MN, Peluffo G, Taylor MC, Kelly JM, Wilkinson SR, Radi R. Mitochondrial superoxide radicals mediate programmed cell death in *Trypanosoma cruzi*: cytoprotective action of mitochondrial iron superoxide dismutase overexpression. Biochem. J. 2007; 403:323–334. [PubMed: 17168856]
14. Wolcott RG, Franks BS, Hannum DM, Hurst JK. Bactericidal potency of hydroxyl radical in physiological environments. J. Biol. Chem. 1994; 269:9721–9728. [PubMed: 8144563]
15. Alvarez MN, Piacenza L, Irigoin F, Peluffo G, Radi R. Macrophage-derived peroxynitrite diffusion and toxicity to *Trypanosoma cruzi*. Arch. Biochem. Biophys. 2004; 432:222–232. [PubMed: 15542061]
16. Radi R, Peluffo G, Alvarez MN, Naviliat M, Cayota A. Unraveling peroxynitrite formation in biological systems. Free Radical Biol. Med. 2001; 30:463–488. [PubMed: 11182518]
17. Piacenza L, Peluffo G, Radi R. L-arginine-dependent suppression of apoptosis in *Trypanosoma cruzi*: contribution of the nitric oxide and polyamine pathways. Proc. Natl. Acad. Sci. U.S.A. 2001; 98:7301–7306. [PubMed: 11404465]
18. Bonaldo MC, Souto-Padron T, de Souza W, Goldenberg S. Cell-substrate adhesion during *Trypanosoma cruzi* differentiation. J. Cell. Biol. 1988; 106:1349–1358. [PubMed: 3283152]
19. Denicola A, Rubbo H, Rodriguez D, Radi R. Peroxynitrite-mediated cytotoxicity to *Trypanosoma cruzi*. Arch. Biochem. Biophys. 1993; 304:279–286. [PubMed: 8323293]
20. Panus PC, Wright SA, Chumley PH, Radi R, Freeman BA. The contribution of vascular endothelial xanthine dehydrogenase/oxidase to oxygen-mediated cell injury. Arch. Biochem. Biophys. 1992; 294:695–702. [PubMed: 1567225]
21. Turrens JF, Boveris A. Generation of superoxide anion by the NADH dehydrogenase of bovine heart mitochondria. Biochem. J. 1980; 191:421–427. [PubMed: 6263247]
22. Castro LA, Robalinho RL, Cayota A, Meneghini R, Radi R. Nitric oxide and peroxynitrite-dependent aconitase inactivation and iron-regulatory protein-1 activation in mammalian fibroblasts. Arch. Biochem. Biophys. 1998; 359:215–224. [PubMed: 9808763]
23. Feelisch, DS.; Kubitzek, D.; Werringloer, J. The oxyhemoglobin assay. In: Feelisch, MS.; Stamler, JS., editors. Methods in Nitric Oxide Research. New York: John Wiley & Sons Ltd; 1996. p. 455-478.
24. Brito C, Naviliat M, Tiscornia AC, Vuillier F, Gualco G, Dighiero G, Radi R, Cayota AM. Peroxynitrite inhibits T lymphocyte activation and proliferation by promoting impairment of tyrosine phosphorylation and peroxynitrite-driven apoptotic death. J. Immunol. 1999; 162:3356–3366. [PubMed: 10092790]
25. Woo HA, Kang SW, Kim HK, Yang KS, Chae HZ, Rhee SG. Reversible oxidation of the active site cysteine of peroxiredoxins to cysteine sulfinic acid. Immunoblot detection with antibodies specific for the hyperoxidized cysteine-containing sequence. J. Biol. Chem. 2003; 278:47361–47364. [PubMed: 14559909]
26. Detweiler CD, Deterding LJ, Tomer KB, Chignell CF, Germolec D, Mason RP. Immunological identification of the heart myoglobin radical formed by hydrogen peroxide. Free Radical Biol. Med. 2002; 33:364–369. [PubMed: 12126758]
27. Romero N, Radi R, Linares E, Augusto O, Detweiler CD, Mason RP, Denicola A. Reaction of human hemoglobin with peroxynitrite. Isomerization to nitrate and secondary formation of protein radicals. J. Biol. Chem. 2003; 278:44049–44057. [PubMed: 12920120]
28. Radi R, Beckman JS, Bush KM, Freeman BA. Peroxynitrite oxidation of sulfhydryls. The cytotoxic potential of superoxide and nitric oxide. J. Biol. Chem. 1991; 266:4244–4250. [PubMed: 1847917]
29. Chevallet M, Wagner E, Luche S, van Dorsselaer A, Leize-Wagner E, Rabilloud T. Regeneration of peroxiredoxins during recovery after oxidative stress: only some overoxidized peroxiredoxins

can be reduced during recovery after oxidative stress. J. Biol. Chem. 2003; 278:37146–37153. [PubMed: 12853451]

30. Radi R, Cassina A, Hodara R, Quijano C, Castro L. Peroxynitrite reactions and formation in mitochondria. Free Radical Biol. Med. 2002; 33:1451–1464. [PubMed: 12446202]
31. Poderoso JJ, Carreras MC, Lisdero C, Riobo N, Schopfer F, Boveris A. Nitric oxide inhibits electron transfer and increases superoxide radical production in rat heart mitochondria and submitochondrial particles. Arch. Biochem. Biophys. 1996; 328:85–92. [PubMed: 8638942]
32. Wilkinson SR, Horn D, Prathalingam SR, Kelly JM. RNA interference identifies two hydroperoxide metabolizing enzymes that are essential to the bloodstream form of the African trypanosome. J. Biol. Chem. 2003; 278:31640–31646. [PubMed: 12791697]
33. Barr SD, Gedamu L. Role of peroxidoxins in *Leishmania chagasi* survival. Evidence of an enzymatic defense against nitrosative stress. J. Biol. Chem. 2003; 278:10816–10823. [PubMed: 12529367]
34. Finzi JK, Chiavegatto CW, Corat KF, Lopez JA, Cabrera OG, Mielniczki-Pereira AA, Colli W, Alves MJ, Gadelha FR. *Trypanosoma cruzi* response to the oxidative stress generated by hydrogen peroxide. Mol. Biochem. Parasitol. 2004; 133:37–43. [PubMed: 14668010]
35. Thomson L, Denicola A, Radi R. The trypanothione-thiol system in *Trypanosoma cruzi* as a key antioxidant mechanism against peroxynitrite-mediated cytotoxicity. Arch. Biochem. Biophys. 2003; 412:55–64. [PubMed: 12646268]
36. Bryk R, Griffin P, Nathan C. Peroxynitrite reductase activity of bacterial peroxiredoxins. Nature. 2000; 407:211–215. [PubMed: 11001062]
37. Quijano C, Romero N, Radi R. Tyrosine nitration by superoxide and nitric oxide fluxes in biological systems: modeling the impact of superoxide dismutase and nitric oxide diffusion. Free Radical Biol. Med. 2005; 39:728–741. [PubMed: 16109303]
38. Poderoso JJ, Lisdero C, Schopfer F, Riobo N, Carreras MC, Cadenas E, Boveris A. The regulation of mitochondrial oxygen uptake by redox reactions involving nitric oxide and ubiquinol. J. Biol. Chem. 1999; 274:37709–37716. [PubMed: 10608829]
39. Muñoz-Fernandez MA, Fernandez MA, Fresno M. Activation of human macrophages for the killing of intracellular *Trypanosoma cruzi* by TNFα and IFNγ through a nitric oxide-dependent mechanism. Immunol. Lett. 1992; 33:35–40. [PubMed: 1330900]
40. Villalta F, Zhang Y, Bibb KE, Kappes JC, Lima MF. The cysteine-cysteine family of chemokines RANTES, MIP-1α, and MIP-1β induce trypanocidal activity in human macrophages via nitric oxide. Infect. Immun. 1998; 66:4690–4695. [PubMed: 9746565]
41. Alvarez MN, Trujillo M, Radi R. Peroxynitrite formation from biochemical and cellular fluxes of nitric oxide and superoxide. Methods Enzymol. 2002; 359:353–366. [PubMed: 12481586]

Europe PMC Funders Author Manuscripts

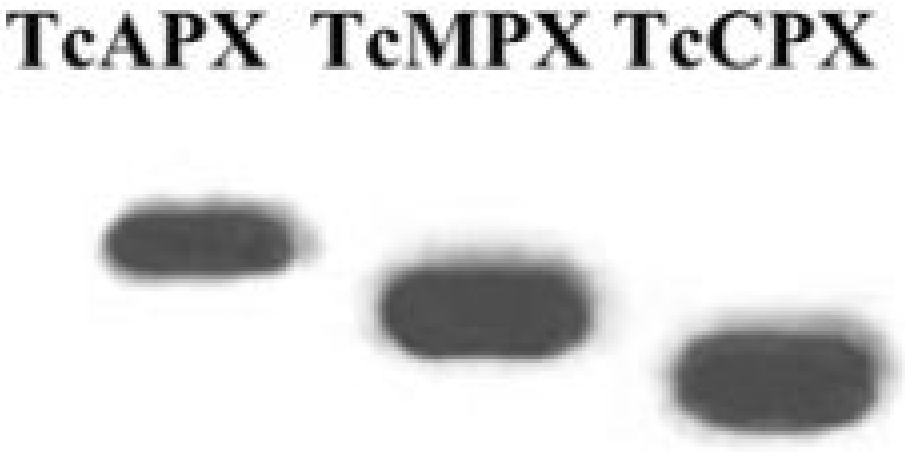

Figure 1. Expression of TcAPX, TcMPX and TcCPX in transformed epimastigotes

Total cell extracts (25 μg) from *T. cruzi* epimastigotes transformed to overexpress TcAPX, TcMPX or TcCPX [11,12] were run on SDS/PAGE (13 % gels) and transferred on to nitrocellulose membranes. Equal loading was checked by Ponceau-S red staining of the membranes. Blots were probed with a monoclonal anti-c-Myc antibody (9E10) that recognized epitope-tagged TcAPX, TcMPX and TcCPX. Enzyme activity in overexpressing cells is 5-, 1.9- and 2.5-fold higher for TcAPX, TcMPX and TcCPX respectively [11,12].

Europe PMC Funders Author Manuscripts

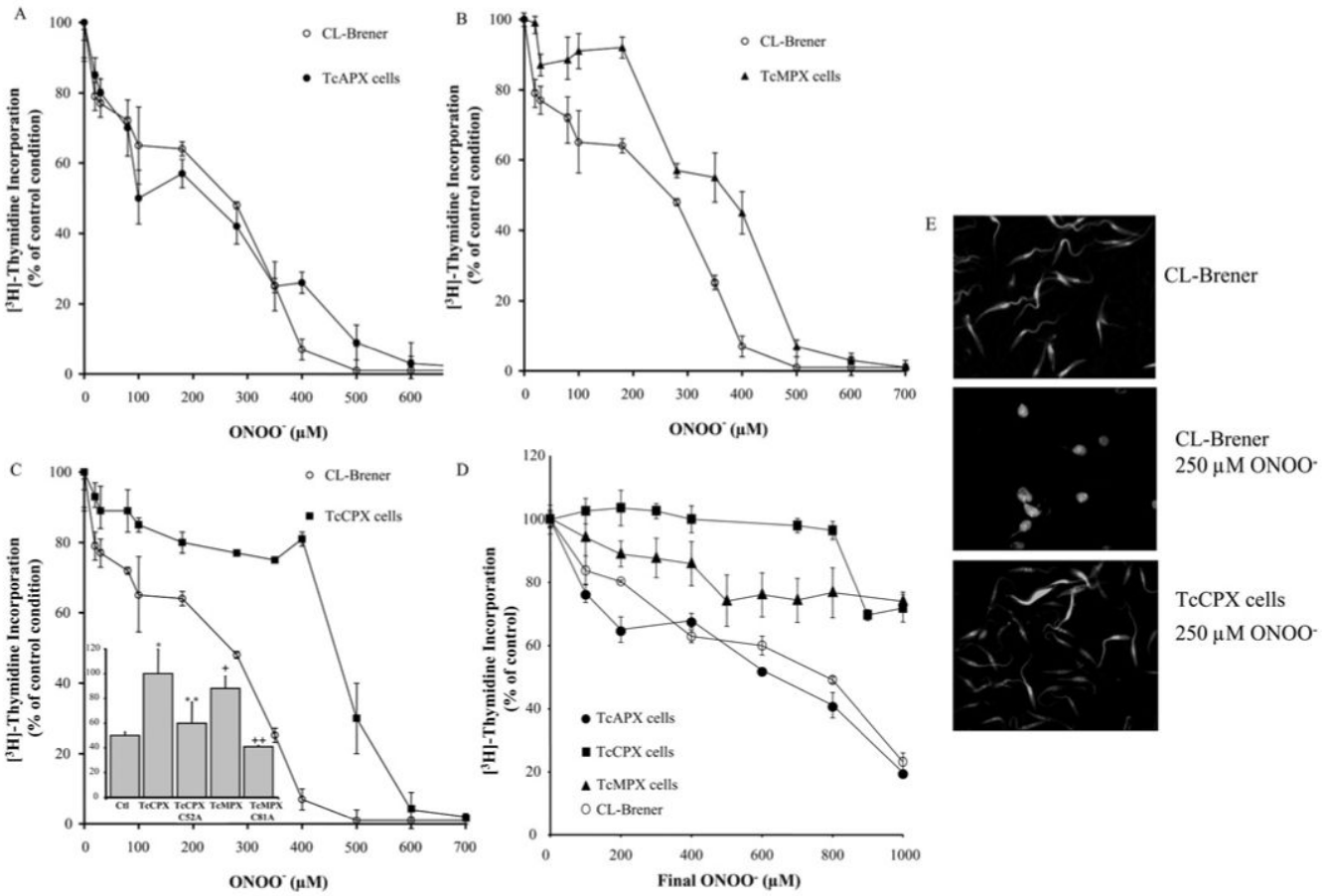

Figure 2. Susceptibility of transformed and wild-type *T. cruzi* epimastigotes to peroxynitrite challenge

Parasites (3×10^8 cells · ml^{-1}) were exposed to a single dose of peroxynitrite ($ONOO^-$, 0-700 μM) under vortex-mixing. After treatment, cells (5×10^6) were cultured in BHI medium and pulsed with 1 μCi [^{3}H]thymidine for 18 h at 28°C. After incubation, cells were harvested and assayed for incorporated radioactivity. Results are percentage [^{3}H]thymidine incorporation compared with control conditions (no peroxynitrite addition) for each cell line. (**A**) Control (CL-Brener, wild-type) compared with TcAPX cells, (**B**) control (CL-Brener) compared with TcMPX cells and (**C**) control (CL-Brener) compared with TcCPX cells. Inset: *T. cruzi* epimastigotes [control (Ctl; CL-Brener), TcCPX or TcMPX overexpressing cells, and TcCPX C52A and TcMPX C81A; 3×10^8 cells · ml^{-1}] were exposed to a single dose of 300 μM peroxynitrite. Cell viability was evaluated as in (**A**) and results are percentage [^{3}H]thymidine incorporation compared with control conditions (no peroxynitrite addition) for each cell line (*y*-axis). **, $P < 0.05$ compared with * and ++, $P < 0.05$ compared with +. (**D**) Parasites (3×10^8 cells · ml^{-1}) [CL-Brener (wild-type), TcAPX, TcCPX or TcMPX overexpressing cells] were exposed to consecutive doses of 100 μM peroxynitrite ($ONOO^-$) to the final peroxynitrite concentrations indicated (0-1000 μM). Parasite viability was evaluated as in (**A**) and results are expressed as percentage [^{3}H]thymidine incorporation compared with control conditions (no peroxynitrite addition) for each cell line. (**E**) 6-CFDA (10 μM) pre-loaded CL-Brener (wild-type) and TcCPX parasites (3×10^8 cells · ml^{-1}) were exposed to a single dose of 250 μM peroxynitrite ($ONOO^-$) and cell morphology was evaluated by epifluorescence microscopy (×60).

Europe PMC Funders Author Manuscripts

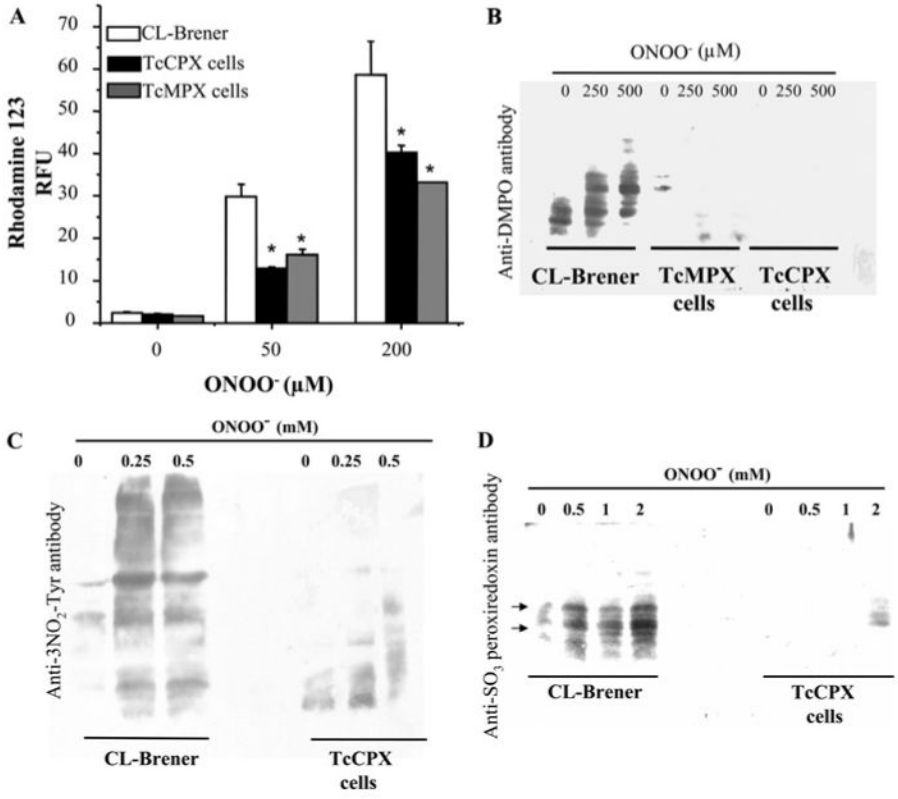

Figure 3. Peroxynitrite-dependent protein modifications in transformed and wild-type *T. cruzi*

(**A**) Detection of intracellular DHR oxidation. DHR (50 μM) pre-loaded *T. cruzi* epimastigotes [wild-type (CL-Brener), TcMPX or TcCPX overexpressing cells; 3×10^8 cells $\cdot$ ml^{-1}] were exposed to a single dose of 50 and 200 μM peroxynitrite ($ONOO^-$). Parasites were washed in DPBS and 3×10^7 cells were used to measure intracellular RH 123 at λ_{ex} = 485 nm and λ_{em} = 590 nm. Results are arbitrary fluorescence units and are means ± S.D. (n = 3). *, $P < 0.001$ compared with wild-type cells. (**B**) Detection of DMPO-protein adducts. Epimastigotes [wild-type (CL-Brener), TcMPX or TcCPX overexpressing cells; 3×10^8 cells $\cdot$ ml^{-1}] pre-loaded with DMPO (100 mM) were treated with peroxynitrite ($ONOO^-$, 0-0.5 mM). After treatment, equal amounts of cell extracts (50 μg) were run on SDS/PAGE (13% gels). Equal loading was checked by Ponceau-S red staining of the transferred nitrocellulose membranes before Western blot analysis using anti-DMPO-nitrone antibody. (**C**) Protein 3-nitrotyrosine detection. Wild-type (CL-Brener) and TcCPX overexpressing epimastigotes (3×10^8 cells $\cdot$ ml^{-1}) were treated with peroxynitrite ($ONOO^-$, 0-0.5 mM) and washed. After treatment equal amounts of cell extracts (50 μg) were run on SDS/PAGE (13% gels). Equal loading was checked by Ponceau-S red staining of the transferred nitrocellulose membranes before Western blot analysis using a polyclonal anti-nitrotyrosine ($3NO_2$-Tyr) antibody as described in the Experimental section. (**D**) Detection of sulfonylated peroxiredoxins. Wild-type and TcCPX overexpressing epimastigotes (3×10^8 cells $\cdot$ ml^{-1}) were treated with peroxynitrite ($ONOO^-$, 0-2 mM) and processed for Western blot analysis as in (**B**) using the polyclonal anti-[sulfonic (SO_3) peroxiredoxin)] antibody. Arrows indicate the bands compatible with over-oxidized TcCPX (~21 kDa) and TcMPX (~25 kDa) *T. cruzi* peroxiredoxins [11].

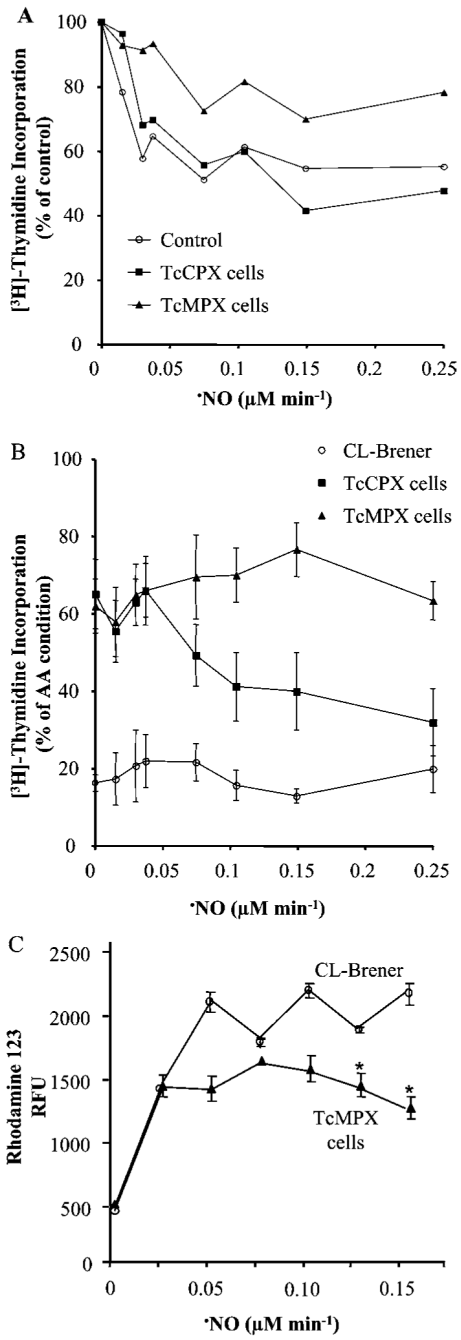

Figure 4. Susceptibility of transformed and wild-type *T. cruzi* epimastigotes to $^{\bullet}NO$ and $O_2^{\bullet-}$ fluxes

(**A**) Wild-type (CL-Brener, Control), TcMPX or TcCPX overexpressing epimastigotes (3×10^8 cells $\cdot$ ml^{-1}) were treated in BHI medium with different concentrations of the $^{\bullet}NO$ donor NOC-18 (0-0.25 μM $^{\bullet}NO \cdot$ min^{-1}). Parasites were then seeded at a cell density of 5×10^6 cells/200 μl BHI medium and pulsed with 1 μCi [^{3}H]thymidine for 18 h at 28°C. After incubation, cells were harvested and assayed for radioactivity. Results are percentage of [^{3}H]thymidine incorporation compared with the control (no addition of NOC-18) for each cell line. (**B**) Wild-type (CL-Brener) and TcMPX overexpressing parasites (3×10^8 cells $\cdot$ ml^{-1}) were treated with AA (5 μM) in the presence or absence of different concentrations of

NOC-18 (0-0.25 μM $^{\bullet}$NO · min^{-1}). Results are percentage of [^{3}H]thymidine incorporation compared with non-treated cells (taken as 100 %). Parasite viability was performed as in (**A**). (**C**) DHR (50 μM) pre-loaded CL-Brener (wild-type) and TcMPX overexpressing cells were treated with AA (5 μM) and different concentrations of spermidine NONOate (0-0.15 μM · $^{\bullet}$NO min^{-1}) for 1 h in DPBS pH 7.3 at 28°C. After incubation, detection of RH 123 was evaluated fluorometrically (λ_{ex} = 485 nm and λ_{em} = 590 nm) as described in the Experimental section. Results are expressed as arbitrary fluorescence units (RFU) and are means ± S.D. (n = 3). *, P < 0.01 compared with wild-type cells.

Europe PMC Funders Author Manuscripts

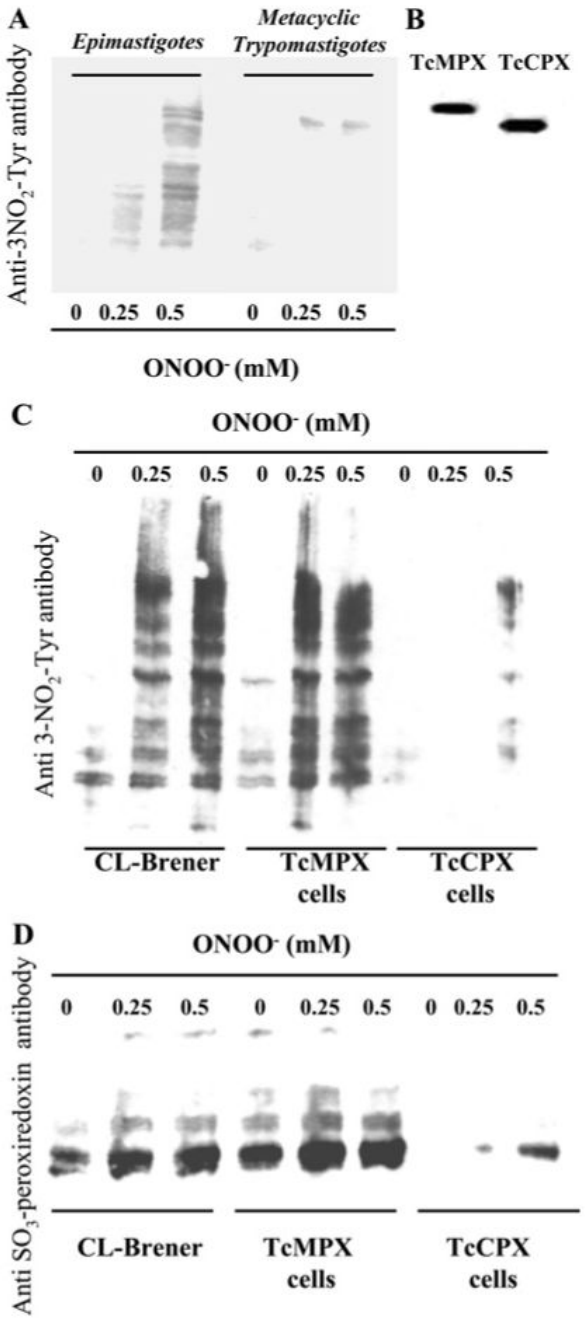

Figure 5. Detection of protein 3-nitrotyrosine and sulfonylated peroxiredoxins in peroxynitrite-treated metacyclic trypomastigotes

(**A**) Wild-type (CL-Brener) epimastigotes and metacyclic trypomastigotes (3×10^8 cells · ml^{-1}) were exposed to peroxynitrite ($ONOO^-$, 0-0.5 mM) and washed in DPBS. After treatment, equal amounts of cell extracts (50 μg) were run on SDS/PAGE (13% gels). Equal loading was checked by Ponceau-S red staining of the transferred nitrocellulose membranes before Western blot analysis using a polyclonal anti-nitrotyrosine ($3NO_2$-Tyr) antibody, as described in the Experimental section. (**B**) Metacyclic trypomastigotes from TcMPX or TcCPX overexpressing cells were generated by chemical differentiation (as described in the Experimental section). Following 96 h incubation, parasites were centrifuged at 800 ***g*** for 10

Europe PMC Funders Author Manuscripts

min at 25°C and washed three times in DPBS. After treatment, equal amounts of cell extracts (25 μg) were run on SDS/PAGE (13% gels). Equal loading was checked by Ponceau-S red staining of the transferred nitrocellulose membranes before Western blot analysis using a monoclonal anti-c-Myc antibody (9E10) for detection of the epitope-tagged proteins in TcMPX and TcCPX. (**C**) Wild-type (CL-Brener), TcMPX or TcCPX overexpressing metacyclic trypomastigoes (3×10^8 cells $\cdot$ ml^{-1}) were exposed to peroxynitrite ($ONOO^-$, 0-0.5 mM) and washed in DPBS. After treatment, equal amounts of cell extracts (50 μg) were run on SDS/PAGE (13% gels). Equal loading was checked by Ponceau-S red staining of the transferred nitrocellulose membranes before Western blot analysis using a polyclonal anti-nitrotyrosine ($3NO_2$-Tyr) antibody as described in the Experimental section. (**D**) Wild-type, TcMPX or TcCPX overexpressing metacyclic trypomastigoes (3×10^8 cells $\cdot$ ml^{-1}) were exposed to peroxynitrite ($ONOO^-$, 0-0.5 mM) and processed for Western blot analysis as in (**C**) using the polyclonal anti-[sulfonic (SO_3) peroxiredoxin] antibody.

Table 1

Differential susceptibility of wild-type and TcCPX, TcMPX or TcAPX overexpressing epimastigotes to H_2O_2 and peroxynitrite challenge

Parasites (3×10^8 cells $\cdot$ ml^{-1}) were exposed in DPBS to different concentrations of H_2O_2 or peroxynitrite ($ONOO^-$) (0-1000 μM) for 1 h at 28°C. After treatment, 5×10^6 cells were cultured in 200 μl BHI medium and pulsed with 1μCi [^{3}H]thymidine for 18 h at 28°C, harvested and assayed for incorporated radioactivity. The IC_{50} value (μM), corresponding to the inhibition of [^{3}H]thymidine incorporation by 50%, was determined. Results are means ± S.D. ($n = 3$). *$P < 0.05$ for H_2O_2 and $ONOO^-$ conditions

Cell line	H_2O_2 IC_{50}	$ONOO^-$ IC_{50}
CL-Brener	213 ± 18*	280 ± 25
TcMPX	294 ± 15	400 ± 15*
TcCPX	300 ± 16	480 ± 18*
TcAPX	425 ± 11*	250 ± 12

Table 2

Susceptibility of transformed cells to macrophage-derived $^{\bullet}NO$ and $O_2^{\bullet-}$ fluxes

Wild-type (CL-Brener), and TcAPX, TcMPX or TcCPX overexpressing (3×10^8 cells $\cdot$ ml^{-1}) epimastigotes were co-cultured in a cell-to-cell contact model with macrophages stimulated to produced $O_2^{\bullet-}$ (PMA activation), $^{\bullet}NO$ [IFNγ (interferon γ) plus lipopolysaccharide stimulation] or $O_2^{\bullet-}$ and $^{\bullet}NO$ for 90 min at 37°C. After incubation, epimastigotes were collected by centrifugation at 800 ***g*** for 10 min at 25°C, washed in DPBS and aliquots containing 5×10^6 parasites used for [^{3}H]thymidine incorporation assays. Results are the percentage of [^{3}H]thymidine incorporation compared with the control condition (non-activated macrophages) and are means ± S.D. (n=3). **, $P < 0.05$ compared with wild-type cells (*)

	Percentage [^{3}H]thymidine incorporation			
Cell line	**Control**	**$O_2^{\bullet-}$**	**$^{\bullet}NO$**	**$O_2^{\bullet-}$+$^{\bullet}NO$**
CL-Brener	100 ± 5	100 ± 7	100 ± 4	50 ± 5*
TcAPX	100 ± 7	87 ± 7	81 ± 10	44 ± 7
TcMPX	100 ± 10	80 ± 5	67 ± 2	80 ± 4**
TcCPX	100 ± 9	110 ± 3	97 ± 2	112 ± 7**